

# Early Paleozoic orogenic collapse, tectonic stability, and late Paleozoic continental rifting revealed through thermochronology of K-feldspars, southern Norway

W. J. Dunlap

Research School of Earth Sciences, The Australian National University, Canberra ACT

H. Fossen

Department of Geology, University of Bergen, Bergen, Norway

**Abstract.** Southern Norway was subjected to contractional orogenesis and subsequent extensional collapse during the early to middle Paleozoic when Baltica collided with Laurentia, resulting in the Caledonian Orogen. The largely unknown post-Caledonian Paleozoic thermal history of the crust in southern Norway has been assessed through application of multiple diffusion domain thermal modeling of K-feldspar  $^{40}\text{Ar}/^{39}\text{Ar}$  data. Samples were collected along a 250 km E-W traverse from the internides of the orogen along the western coast near Bergen through a series of middle to upper crustal nappes to the east. The K-feldspar thermal models, which complement published mica and hornblende  $^{40}\text{Ar}/^{39}\text{Ar}$  data, are consistent with rapid cooling at the end of the Caledonian orogenic cycle, when Early Devonian (~400 Ma) extensional collapse resulted in exhumation through mainly midcrustal conditions. Following extensional collapse, a period of relative tectonic and thermal stability may have prevailed until ~300 Ma. The K-feldspar modeling suggests that southern Norway entered a new phase of relatively rapid cooling (a few  $^{\circ}\text{C}/\text{Ma}$ ) in the Permian-Carboniferous and that the increase in cooling rate was diachronous across the traverse. The onset of this cooling phase occurs at about the time of the earliest faulting and magmatism in the Oslo Graben to the southeast. The increase in cooling rate may also indirectly date the onset of the first important rift phase and associated sedimentation in the North Sea graben system. The distribution of Permian and younger fission track ages in both southern continental Norway and its marginal basin sediments is consistent with the Permian-Carboniferous rapid cooling recorded in the K-feldspars. The simplest explanation for the late Paleozoic increase in cooling rate is that rifting around the margin of southern Norway has resulted in a decrease in the base level and an increase in the rate of erosional denudation, resulting in essentially uniform exhumation of ~2-4 km along the traverse.

## 1. Introduction

Development of the Caledonian Orogen in SW Scandinavia has been shown to consist of both a multiphase crustal thickening history (~450-410 Ma) and a subsequent extensional collapse phase [Andersen *et al.*, 1991; Fossen, 1992]. The relative ages of individual phases of deformation

are distinguishable from overprinting relationships and kinematic studies, and the absolute timing of these phases has recently been explored through  $^{40}\text{Ar}/^{39}\text{Ar}$  geochronology [Chauvet and Dallmeyer, 1992; Dallmeyer *et al.*, 1992; Boundy *et al.*, 1996; Fossen and Dunlap, 1998]. However, the postorogenic (late Paleozoic) exhumation history of the region is largely unknown, mostly because of the almost complete absence of post-Middle Devonian sediments outside of the Oslo Graben [Neumann *et al.*, 1992; Olausson *et al.*, 1994; see also Fossen *et al.*, 1997].

The  $^{40}\text{Ar}/^{39}\text{Ar}$  dating method is useful for unraveling the thermal evolution of the crust where there is little stratigraphic or tectonometamorphic control. In southern Norway,  $^{40}\text{Ar}/^{39}\text{Ar}$  dating of micas and amphiboles indicates that thrusting of major Caledonian nappes was not completed before the earliest Devonian (timescale from Gradstein and Ogg [1996]), that is, shortly before the onset of extensional reactivation of the thrusts at about 400 Ma [Fossen and Dunlap, 1998]. This thermochronological information is, however, generally restricted to temperatures in excess of about 300 $^{\circ}\text{C}$ , and in Norway the record revealed by this method ends at ~380-400 Ma. A relatively new tool in this respect is multiple diffusion domain (MDD) analysis of argon outgassed from K-feldspars, which provides important thermochronological information through the temperature interval of ~350 $^{\circ}$ -150 $^{\circ}\text{C}$  [e.g., Lovera *et al.*, 1991]. In southwestern Norway this temperature interval corresponds to the time gap between Early Devonian extensional collapse and Mesozoic apatite fission track ages [e.g., Rohrman *et al.*, 1996]. In this work we apply K-feldspar  $^{40}\text{Ar}/^{39}\text{Ar}$  thermochronology in combination with geologic constraints to explore the middle to late Paleozoic thermal history of the southern Norwegian crust.

## 2. Geologic Setting

The geology of southern Norway (Figure 1) is dominated by a variety of Precambrian igneous and metamorphic basement rocks of mainly Proterozoic age forming the Baltic Shield, the Western Gneiss Region (WGR), and the Caledonian allochthonous nappes. The basement has been involved in several orogenic cycles [Gorbatshev, 1985], the most important occurring at ~1500-1400 Ma, 1250-850 Ma (Sveconorwegian-Grenvillian Orogeny), and ~450-400 Ma (Caledonian Orogeny).

Copyright 1998 by the American Geophysical Union.

Paper number 98TC01603.  
0278-7407/98/98TC-01603\$12.00

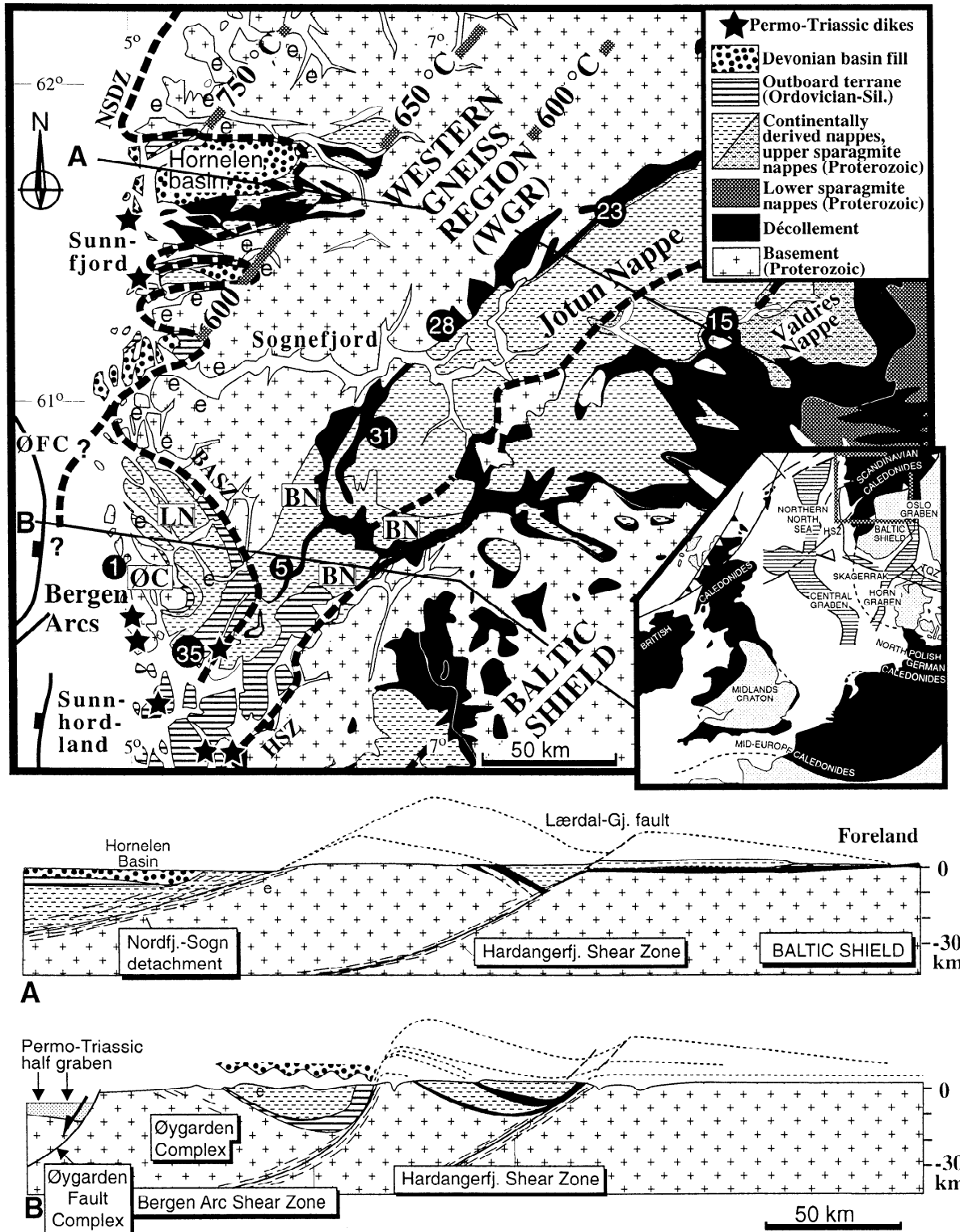


**Figure 1.** Geologic map, showing main tectonic units and sampling localities (sample numbers in solid circles, prefix N omitted). Two profiles illustrate the large-scale overprint of thrusting/contractional structures by late Caledonian extensional deformation. Floating Devonian section is exposed in northernmost Bergen Arc system (not shown on map). Temperature contours in the Western Gneiss Region (WGR) are adapted from *Griffin et al.* [1985]. Abbreviations are as follows: BASZ, Bergen Arcs Shear Zone; BN, Bergsdalen Nappes; HSZ, Hardangerfjord shear zone; LN, Lindås Nappe; NSDZ, Nordfjord-Sogn detachment zone; ØC, Øygarden Complex; ØFC, Øygarden Fault Complex. "Sparagmite" is defined in text.

Upper Proterozoic to Cambrian sedimentary sequences were deposited on this basement during a period of continental rifting which began about 800 Ma [e.g., *Kumpulainen and Nystuen*, 1985]. A sequence of coarse clastic fluvial deposits are overlain by glacial deposits (~650 Ma) and, in turn, by a fluvial-marine sequence deposited during continued subsidence of the craton ("sparagmites", in Figure 1). These sediments are preserved in Caledonian thrust nappes, and simple restoration indicates deposition in a rift system west of the present Norwegian coastline [*Kumpulainen and Nystuen*, 1985]. The depositional contact with the basement (e.g., base of Jotun Nappe) indicates that at least parts of these nappes were near the surface well before 650 Ma. A stable platform setting was achieved by Cambrian times, but this entire sedimentary package was subsequently overthrust during Caledonian orogenesis.

The Caledonian Orogeny is interpreted to have culminated in a continent-continent collision when the western edge of Baltica was subducted beneath the Laurentian plate. This interpretation is supported by thermobarometric data from eclogite-coesite-bearing rocks which formed about  $425 \pm 25$  Ma in the western portions of the WGR [e.g., *Gebauer et al.*, 1985; *Griffin et al.*, 1985; *Dallmeyer et al.*, 1992]. The impact of the Caledonian Orogeny on Baltica increases to the west, and the WGR and the Øygarden Complex show evidence of heterogeneous and locally intense Caledonian reworking.

During the Caledonian convergent history an orogenic wedge was accreted onto Baltica, the remnants of which are preserved in a well-exposed and up to 350 km wide orogenic belt (Figure 1, inset). The Jotun Nappe, which apparently represents a detached fragment of the precollisional continental margin of Baltica, was thrust for several hundred kilometers to the southeast over the WGR [*Hossack and Cooper*, 1986]. In addition to this continental derivative the upper and western thrust nappes (Bergen Arcs) include exotic fragments of ophiolite and island arc complexes. The sedimentary cover on the peneplanized Baltic craton acted as a mechanically weak décollement during nappe translations. The  $^{40}\text{Ar}/^{39}\text{Ar}$  studies of amphiboles and micas in southwestern Norway [*Chauvet and Dallmeyer*, 1992; *Boundy et al.*, 1996; *Fossen and Dunlap*, 1998] indicate (1) a ~450 Ma cooling history for some of the tectonostratigraphically highest and most exotic nappes [cf. *Berry et al.*, 1995], (2) cooling through ~500°C in the western basement at 400-410 Ma, and (3) exhumation of this basement and the lower nappes through ~350°C at about 400 Ma.

A change from Caledonian crustal thickening to extensional collapse shortly before 400 Ma [*Fossen and*

*Dunlap*, 1998] was marked by reactivation of the basal décollement of the orogenic wedge as a low-angle west directed normal shear zone, with coincident formation of steeper west and NW dipping extensional shear zones and faults (Nordfjord-Sogen detachment zone (NSDZ), Bergen Arcs Shear Zone (BASZ), and Hardangerfjord Shear Zone (HSZ) in the WGR) [*Fossen and Rykkelid*, 1992]. Displacement along these latter zones varies from several kilometers (HSZ) to many tens of kilometers (NSDZ). Rapid decompression and cooling as a result of the extensional deformation was accompanied by deposition of Devonian conglomerates and sandstones upon the WGR [*Norton*, 1986; *Chauvet and Dallmeyer*, 1992; *Osmundsen and Andersen*, 1994; *Boundy et al.*, 1996]. In the Jotun Nappe region, *Fossen and Dunlap* [1998] found two populations of  $^{40}\text{Ar}/^{39}\text{Ar}$  ages which, through kinematic and textural analysis, indicate thrusting of the Jotun Nappe at ~415-409 Ma and reactivation of the thrust as a low-angle west directed décollement at ~400 Ma, contemporaneous with exhumation of Baltica in the coastal regions. The youngest  $^{40}\text{Ar}/^{39}\text{Ar}$  ages for micas and amphiboles in southern Norway are ~380 Ma, but cessation of nappe movements likely occurred somewhat earlier.

Subsequent to the Caledonian Orogeny, southern Norway may have experienced relative tectonic stability until about 300 Ma when the Oslo Graben [e.g., *Neumann et al.*, 1992] and possibly also the North Sea rift [*Ziegler*, 1990] began to form. The Oslo Graben is a 400 km long N-S trending rift initiated in a depression which was intruded by magmatic rocks and filled by extrusives and sediments about 300-240 Ma. In contrast, the related North Sea rift system evolved through both Permo-Triassic and Late Jurassic rifting events [e.g., *Færseth et al.*, 1995]. In general, however, the southern Norwegian crust is regarded as one of the major source areas for substantial sediment accumulations in the North Sea and Skagerrak basins during most of the Devonian-Jurassic and Paleocene-Quaternary time intervals [e.g., *Riis*, 1996]. Final cooling of the crust through apatite fission track retention temperatures started in the Triassic and continued in an intermittent fashion into the Neogene, culminating with a domal uplift centered on the present-day topographic high [*Rohrman et al.*, 1995].

### 3. Petrologic and Thermal Constraints on Samples

Seven K-feldspar-bearing samples have been collected along an E-W traverse through southern Norway (Figure 1 and locations in Table 1). The tectonic units sampled are, from

**Table 1.** Sample Location and Type

Sample	Locality	Unit	UTM	Lithology
N1	Toftøy, northwest of Bergen	Øygarden Complex	KN767119	biotite gneiss, top-to-west fabric
N5	Bukkafjell granite	Lower Bergsdalen nappe	LN352177	foliated granite
N15	Kongslknappen, Byggin	Jotun Nappe Complex	MN879001	syenite with semiductile deformation
N17	Nedre Leirungen, south of Gjende	Jotun Nappe Complex	MP904157	granite, deformed
N23	1 km east of Krossbu, Jotunheimen	Valdres sparagmitic	MP490285	sheared arkose with large feldspar clasts
N28	Hafslovatnet, Sogn	Western Gneiss Region	MP035974	quartz-monzonite with K-feldspar augen
N31	Muravatnet, Vikafjellet	Jotun Nappe Complex	LN695635	syenitic gneiss
N35	Danielsvik, south of Bergen	Krossnes granite	KM977784	coarse granite

UTM, universal transverse mercator

east to west, the Jotun Nappe (N15, N23, and N31), the WGR basement (N28), the Bergsdalen Nappes (N5), the Bergen Arcs (N35), and the Øygarden Complex (N1). Below we present petrographic observations and discuss available thermochronology that may bear on the thermal evolution of the K-feldspars that we have analyzed.

The magmatic rocks of the Jotun Nappe formed in the Proterozoic [e.g., *Milnes and Koestler, 1985*] by intrusion of granitic (~1680 Ma) and gabbroic magmas (~1250 Ma [*Schärer, 1980*]). Subsequently, these rocks experienced upper greenschist to amphibolite facies deformation ~900 Ma [*Schärer, 1980*]; we impose this constraint in the modeling below. The sparagmite sediments indicate that portions of the nappe were near the surface prior to the Caledonian orogeny. Caledonian deformation occurred at lower greenschist facies conditions in the southeast (N15) ~415 Ma [*Fossen and Dunlap, 1998*] and at greenschist facies or higher conditions in the northwest (N23, N28, and N31).

Sample N15, from the Proterozoic Kongslknappen syenite near Bygdin, suffered Caledonian deformation in the lower greenschist facies. The thermal peak during this event probably reached about 350°C as most of the white micas yield Caledonian ages [*Fossen and Dunlap, 1998*]. The microstructure of N15 indicates that Caledonian deformation has modified the primary igneous texture. Quartz is partially recrystallized to polygonal grains (~10-50 µm) and new white micas form a weak cleavage. Some K-feldspars are fractured, but preservation of perthitic textures suggests that the grains have not been seriously modified since perhaps 900 Ma.

Sample N23 is a mylonitic arkose from a roadcut near Krossbu. The arkose was deposited in the Proterozoic [e.g., *Bryhni et al., 1983*] but was deformed in Caledonian time under middle greenschist facies conditions. Petrographic analysis indicates that the arkosic protolith suffered SE directed Caledonian deformation. Quartz is entirely recrystallized into equant polygonal grains (100-200 µm), and a pervasive cleavage is formed by white micas. Feldspars are fractured and abraded at their margins, grain interiors exhibit abundant deformation bands, and pressure shadows contain polygonal feldspar grains (~20 µm) that appear to be recrystallized. The dated K-feldspar is dominantly porphyroblast core material.

Sample N31 is from the amphibole-bearing granitic gneiss forming the base of the Jotun Nappe at the Muravatnet Dam. K-feldspar N31 (350-420 µm fragments) is from an unaltered single crystal core of one porphyroblast. Although the rock formed in the amphibolite facies, field relations indicate that this fabric is Proterozoic. Amphibole from this sample exhibits a  $^{40}\text{Ar}/^{39}\text{Ar}$  age spectrum indicative of partial resetting [*Fossen and Dunlap, 1998*], and we believe that temperatures of ~450°C [e.g., *Baldwin et al., 1990*] may have been achieved during Caledonian tectonism.

Sample N28 was collected in the WGR (Figure 1) from the ~976 Ma Hafslo granitoid [*Corfu, 1980*]. Thermometry of eclogite facies mineral parageneses from the WGR suggests that site N28 reached perhaps 550°C during Caledonian orogenesis [*Griffin et al., 1985*]. The granite was slightly deformed and partially retrograded in the greenschist facies and likely reheated in the process, but the K-feldspars do not exhibit significant deformation features. A number of minor

epidote-coated normal faults that accommodated Devonian(?) NW-SE extension occur near (but tens of meters away from) the sample locality. White micas from both the overlying Jotun Nappe and décollement zone yield  $^{40}\text{Ar}/^{39}\text{Ar}$  plateau ages ranging from 400 Ma to 415 Ma [*Fossen and Dunlap, 1998*]. In contrast, one white mica from the WGR several kilometers from site N28 yields a significantly older plateau age of 442 Ma [*Chauvet and Dallmeyer, 1992*]. These data indicate that temperatures of the order of mica closure temperatures (~350°C) were maintained until ~400 Ma, but it is unclear when the ~550°C maximum was reached.

Sample N5 from the Bukkfjell biotite granite in the Lower Bergsdalen Nappe (west of and tectonostratigraphically below the Jotun Nappe) exhibits a macroscopic ductile top-to-the-ESE fabric indicative of deformation in the upper greenschist to lower amphibolite facies. These fabrics are interpreted as Caledonian [*Fossen, 1993*]. Quartz is recrystallized to grain sizes ranging from 50 to 400 µm. Feldspars form either porphyroclasts or masses of recrystallized grains; porphyroclasts dominate the material analyzed here. The porphyroclasts have not been significantly modified since deformation ceased. A biotite plateau age of  $398 \pm 3$  Ma is interpreted as the time of cooling through ~300°-350°C [*Fossen and Dunlap, 1998*], whereas a Rb/Sr age of  $953 \pm 16$  Ma from the same locality is likely to be the age of intrusion [*Pringle et al., 1975*].

Sample N35 was collected from the Krossnes granite of the Bergen Arcs. This granite intruded an island arc setting and crosscut an Ordovician ophiolite suite of the Major Bergen Arc at ~430 Ma (Rb-Sr age [*Fossen and Austrheim, 1988*]) and was subsequently involved in Caledonian upper greenschist to lower amphibolite facies mylonitization, particularly along its northern margin [*Fossen, 1988*]. The ophiolite suite was exposed and covered by sediments of Ashgill-Llandovery age prior to this final Caledonian tectonometamorphic phase. Petrographic examination of K-feldspar N35 reveals that only some minor deformation and alteration (but no recrystallization) occurred after crystallization. The sample locality is from the road section sampled by *Fossen and Austrheim [1988]*.

The Øygarden Complex, where sample N1 was collected, was pervasively deformed and metamorphosed under amphibolite facies conditions during hinterland-directed (top-to-the-W) shearing [*Fossen and Rykkelid, 1990*]. Decreasing temperatures during postcontractual extensional deformation are expressed by a change from ductile deformation to faulting where striated, epidote-coated fault surfaces indicate NW-SE extension [*Fossen, 1998*]. Sample N1 was, however, collected away from such structures to avoid resetting effects. The  $^{40}\text{Ar}/^{39}\text{Ar}$  data from the same locality indicate exhumation and cooling through the closure temperatures of amphiboles and micas no later than 404 Ma and 401 Ma, respectively [*Fossen and Dunlap, 1998*]. However, amphiboles from the same area yield age steps as old as ~450 Ma or older [*Boundy et al., 1996*], which is consistent with a complex preextensional Caledonian thermal history. The microstructure of sample N1 exhibits quartz and feldspars that are recrystallized to coarse polygonal grains (~100-600 µm diameter), and biotite flakes form a pervasive foliation. K-feldspar grains exhibit only minor alteration to sericite.

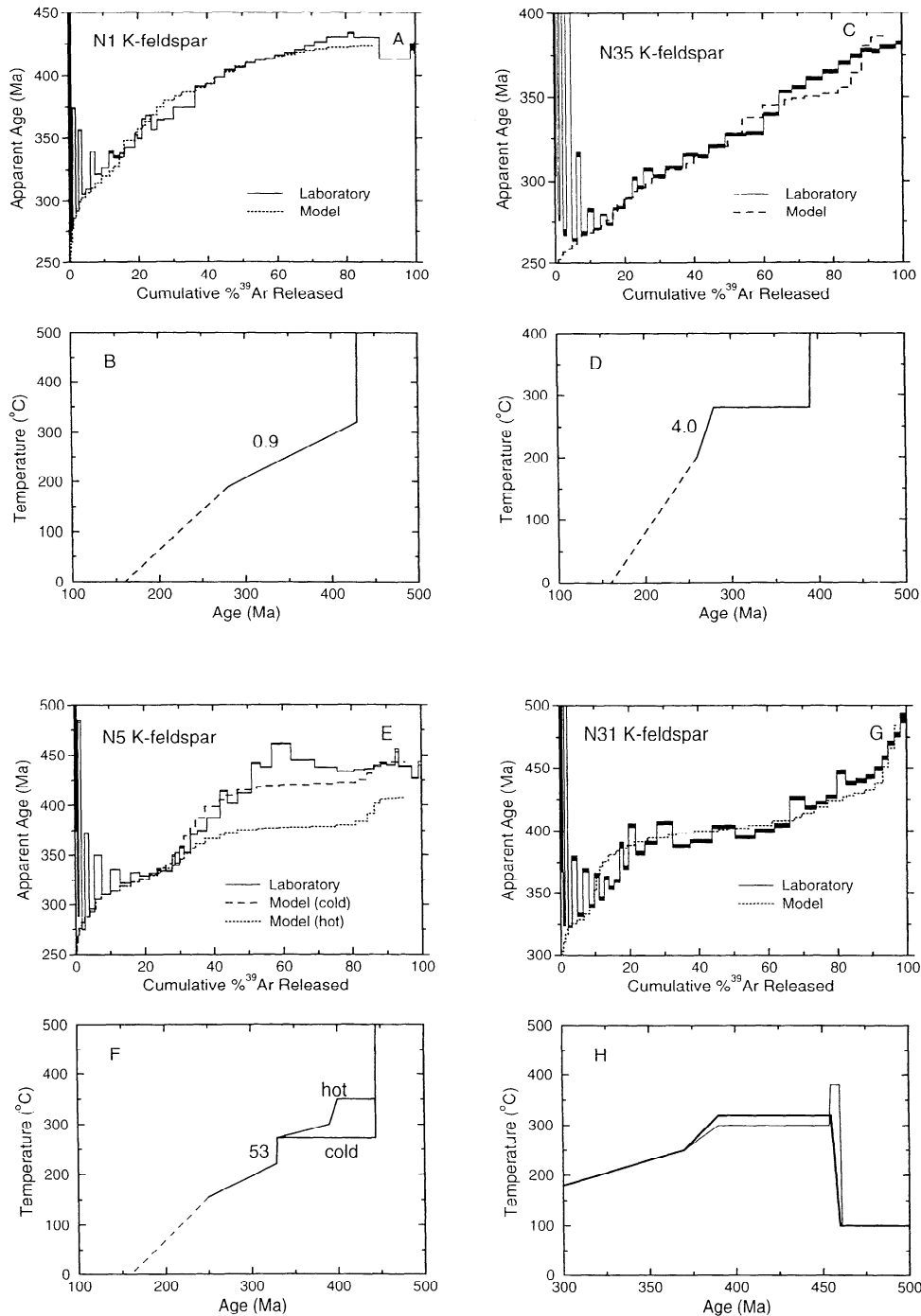


**Figure 2.** Measured and modeled age spectra and preferred thermal histories for K-feldspars: (a) and (b) sample N1, (c) and (d) sample N35, (e) and (f) sample N5, (g) and (h) sample N31, (i) and (j) sample N28, (k) and (l) sample N15, and (m) and (n) sample N23. Figures 2a, 2c, 2e, 2g, 2i, 2k and 2m show calculated age versus fraction of  $^{39}\text{Ar}$  released for laboratory and model results. Figures 2b, 2d, 2f, 2h, 2j, 2l and 2n show time versus temperature plots showing preferred thermal histories used to generate the models in associated age spectrum diagrams. Dashes indicate where inferred.

#### 4. Multiple Diffusion Domain Analysis of K-feldspars

We present below the results of seven  $^{40}\text{Ar}/^{39}\text{Ar}$  step heating experiments performed in the laboratory on K-feldspars extracted from the samples (analytical procedures are identical

to those of Dunlap [1997]). The  $^{40}\text{Ar}/^{39}\text{Ar}$  age spectra for the K-feldspars, plotted in Figure 2 ( $\pm 1\sigma$  errors, excluding error in Figure 2j), are remarkably similar in the range of apparent ages exhibited. In the initial stages of gas release, apparent ages rise from about 250 to 325 Ma in every case to maximum

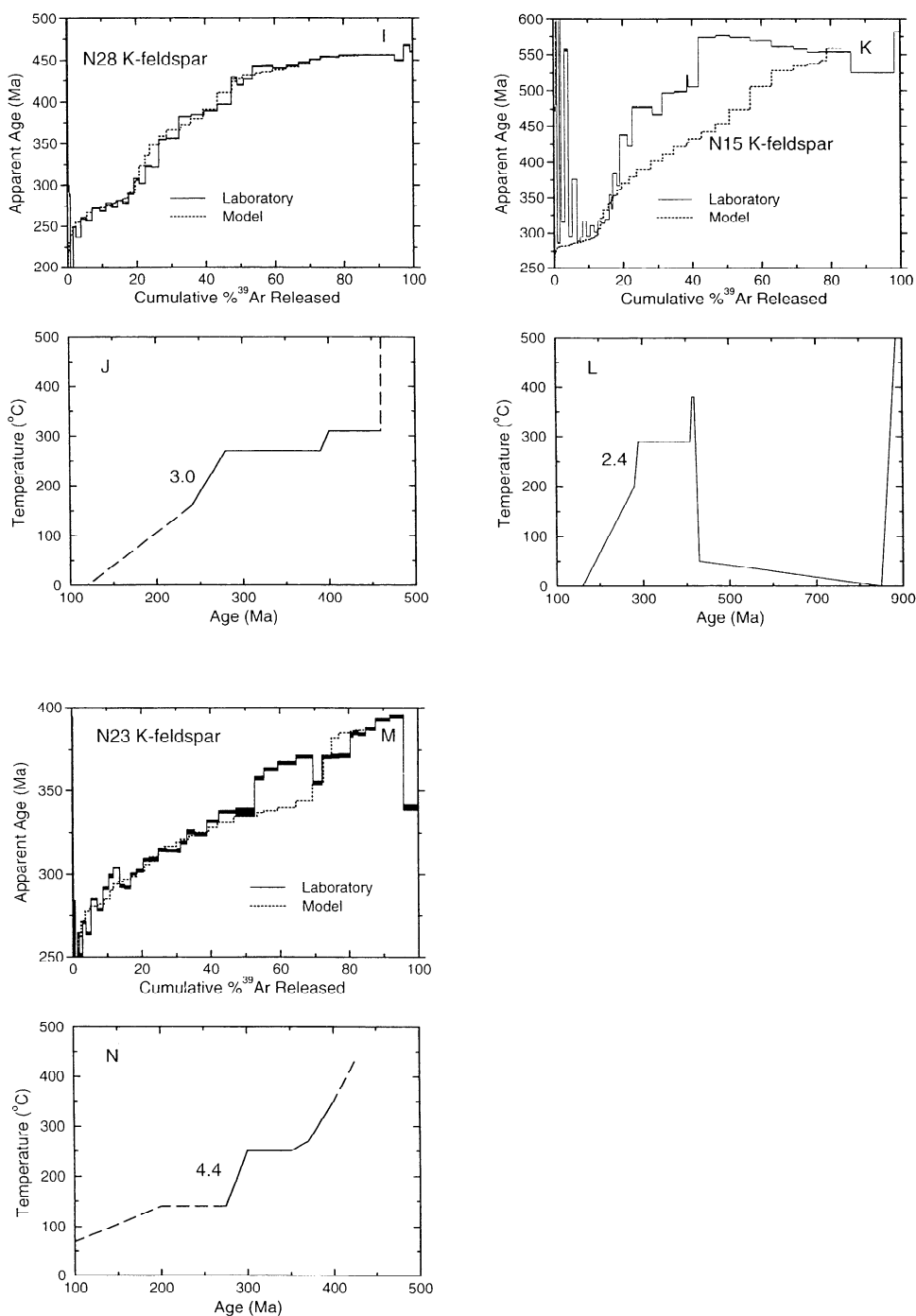


**Figure 2. (continued)**

ages that are Caledonian (~450-380 Ma) or older. This indicates that the K-feldspars were open to argon loss subsequent to Caledonian orogenesis. The K/Ca patterns are complex, with the premelting values generally falling in the range of 20-200, which is typical of K-feldspar.

In this section we also present thermal modeling, effectively an interpretation of the results of  $^{40}\text{Ar}/^{39}\text{Ar}$  step heating experiments. We interpret the results in terms of cooling through a closure temperature range of about 350°-150°C, the typical closure temperature window afforded by K-feldspar if

simple diffusion theory is strictly applicable (for development of this method see *Richter et al.* [1991]). The MDD method assumes that, in both the natural and laboratory situations, the loss or retention of radiogenic argon is from a number of noninteracting domains of variable length scale. The larger the spectrum of length scales within any given K-feldspar, the larger the closure window for argon diffusion will be. For our purposes a single activation energy and a slab geometry for argon diffusion was assumed, and a distribution of model diffusion length scales was calculated. These distributions

were then inverted into time-temperature histories following the method of *Lovera et al.* [1989]. The justification for the MDD procedure, outlined in detail by *Lovera et al.* [1997], is that step heating of K-feldspars commonly reveals dramatic age gradients which cannot be produced by closure of a single domain to diffusive loss of argon [e.g., *McDougall and Harrison, 1988*].

MDD solutions were calculated from the Arrhenius data (see below) using the time, temperature, and fraction of  $^{39}\text{Ar}$  released during the course of the laboratory degassing experiments (see supplementary tables)<sup>1</sup>. Using these MDD solutions, which include a diffusion length scale distribution and a volume fraction for each length scale, preferred thermal paths were calculated by inputting trial thermal histories and minimizing the differences between the measured and modeled age spectra by manual iteration. A "good" fit is that where the measured and modeled age spectra show essentially continuous overlap.

*Harrison et al.* [1993] proposed a formalism by which anomalously old apparent ages in the early stages of gas release (age spikes in first 10-20% of gas release, Figure 2) can be corrected if the release of excess  $^{40}\text{Ar}$  is correlated with chlorine. Using this correlation, if present, parentless chlorine-correlated excess  $^{40}\text{Ar}$  is subtracted from the total radiogenic  $^{40}\text{Ar}$  signal. They suggested that the excess argon is sourced from fluid inclusions. In this study each time the temperature was raised to new heights between 450°C and about 700°C anomalously old apparent ages were produced. This is consistent with the decrepitation of fluid inclusions containing large amounts of excess argon. Two of the seven K-feldspars analyzed here yielded good correlations. The remaining samples did not yield good correlations, the possible causes of which are discussed by *Harrison et al.* [1993].

#### 4.1. Multiple Diffusion Domain Solutions

The MDD solutions were calculated using the method of *Lovera et al.* [1989]. The solutions are shown in Table 2, which lists the diffusion coefficient, the volume fraction of each domain, and their relative sizes. In applying the laboratory heating schedule to these model solutions, we produce a model gas release history that is nearly identical to that measured in the laboratory experiments, although above 1150°C the samples melt (typically after 80-100% of gas release), and no further comparison between the model and laboratory results is possible. The laboratory and model data are presented in Figure 3 in the form of Arrhenius and  $\log r/r_0$  plots [*Lovera et al., 1991*], which allow comparison of the MDD solutions and the laboratory degassing data.

The Arrhenius diagrams are a plot of reciprocal temperature versus  $\log D/r^2$  ( $D$  is effective diffusivity and  $r$  is effective length scale). Isothermal duplicate (or triplicate) runs were performed at 50°C intervals as the temperature was raised from

**Table 2.** Domain Size Distributions

Domain	$\log D_0,$ $\text{cm}^2/\text{s}$	Volume Fraction	Domain Size (Relative)
<i>N15 K-feldspar, <math>E_a = 58.4</math> kcal/mol</i>			
1	10.07	0.02723	0.00005
2	8.926	0.03385	0.00019
3	7.790	0.05033	0.00070
4	5.470	0.05038	0.01007
5	4.711	0.2352	0.02412
6	3.815	0.4262	0.06765
7	1.476	0.1769	1.00000
<i>N23 K-feldspar, <math>E_a = 43.7</math> kcal/mol</i>			
1	6.357	0.07973	0.00012
2	4.870	0.06618	0.00065
3	3.433	0.08503	0.00342
4	2.696	0.4210	0.00798
5	1.400	0.09955	0.03549
6	1.012	0.2105	0.05544
7	-1.500	0.03797	1.00000
<i>N28 K-feldspar, <math>E_a = 52.6</math> kcal/mol</i>			
1	9.597	0.03338	0.00006
2	8.422	0.06883	0.00023
3	7.139	0.06306	0.00100
4	5.210	0.1637	0.00922
5	4.144	0.2159	0.03148
6	3.823	0.00982	0.04555
7	3.304	0.2822	0.08281
8	1.140	0.16305	1.00000
<i>N31 K-feldspar, <math>E_a = 51.1</math> kcal/mol</i>			
1	8.401	0.04589	0.00008
2	7.890	0.03842	0.00014
3	4.590	0.3633	0.00624
4	4.492	0.09166	0.00698
5	3.837	0.3546	0.01484
6	3.031	0.07822	0.03754
7	0.1800	0.02787	1.00000
<i>N5 K-feldspar, <math>E_a = 49.9</math> kcal/mol</i>			
1	9.081	0.02159	0.00005
2	7.860	0.05646	0.00021
3	7.143	0.08820	0.00047
4	6.456	0.03988	0.00104
5	5.835	0.04592	0.00212
6	3.740	0.5452	0.02371
7	2.533	0.1691	0.09520
8	0.4900	0.03363	1.00000
<i>N35 K-feldspar, <math>E_a = 48.7</math> kcal/mol</i>			
1	7.879	0.04634	0.00007
2	6.483	0.08169	0.00037
3	4.221	0.2000	0.00495
4	3.338	0.3673	0.01368
5	3.316	0.1157	0.01402
6	2.185	0.1859	0.05158
7	-0.390	0.00311	1.00000
<i>N1 K-feldspar, <math>E_a = 47.6</math> kcal/mol</i>			
1	6.594	0.02809	0.00446
2	5.875	0.08169	0.01021
3	4.882	0.04872	0.03199
4	4.859	0.00350	0.03286
5	3.782	0.1304	0.11354
6	2.909	0.1507	0.31030
7	2.185	0.3582	0.71387
8	1.892	0.1987	1.00000

$E_a$ , activation energy

<sup>1</sup>Supporting data are available on diskette or via Anonymous FTP from [kosmos.agu.org](http://kosmos.agu.org), director. APEND(Username=anonymous, Password=guest). Diskette may be ordered by mail from AGU, 2000 Florida Ave., NW, Washington, DC 20009 or by phone at 800-966-2481; \$15.00. Payment must accompany order.

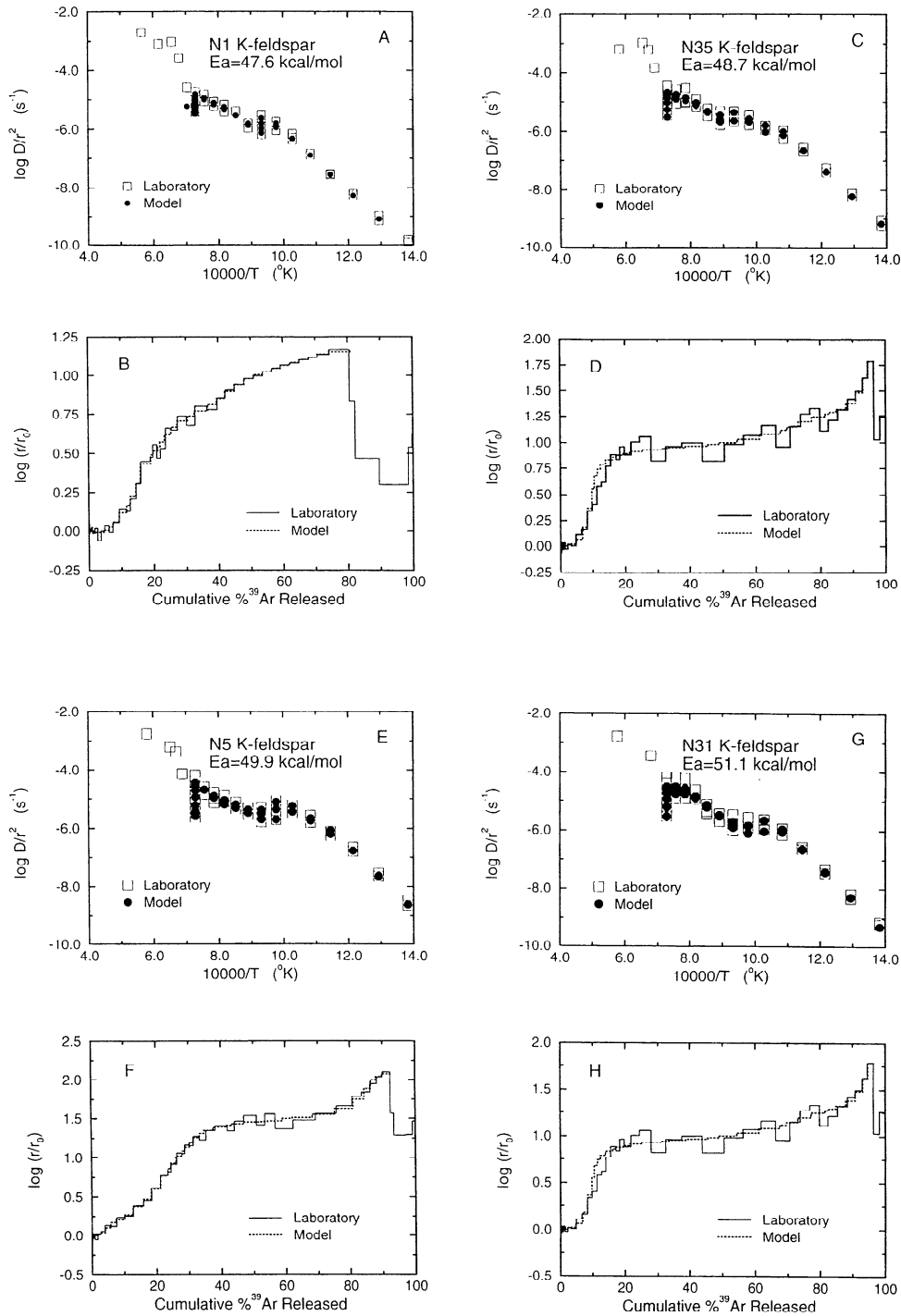


**Figure 3.** Summaries of Arrhenius and  $\log r/r_0$  data for laboratory and model results for seven K-feldspars: (a) and (b) sample N1, (c) and (d) sample N35, (e) and (f) sample N5, (g) and (h) sample N31, (i) and (j) sample N28, (k) and (l) sample N15, and (m) and (n) sample N23. Figures 3a, 3c, 3e, 3g, 3i, 3k and 3m are Arrhenius plots. Laboratory data are calculated using time, temperature, and fraction of <sup>39</sup>Ar released during each step. Model data are calculated by exposing preferred domain distributions (Table 2) to laboratory time-temperature schedule. Activation energies are calculated from best fit least squares regression of first six to eight low-temperature data points; highest activation energy is preferred. Figures 3b, 3d, 3f, 3h, 3j, 3l and 3n are  $\log r/r_0$  plots. These plots track the effective diffusion length scale during the course of the experiment, relative to reference length scale ( $r_0$ ) defined in early portion of gas release. Model data are calculated by exposing domain distributions to laboratory thermal history.



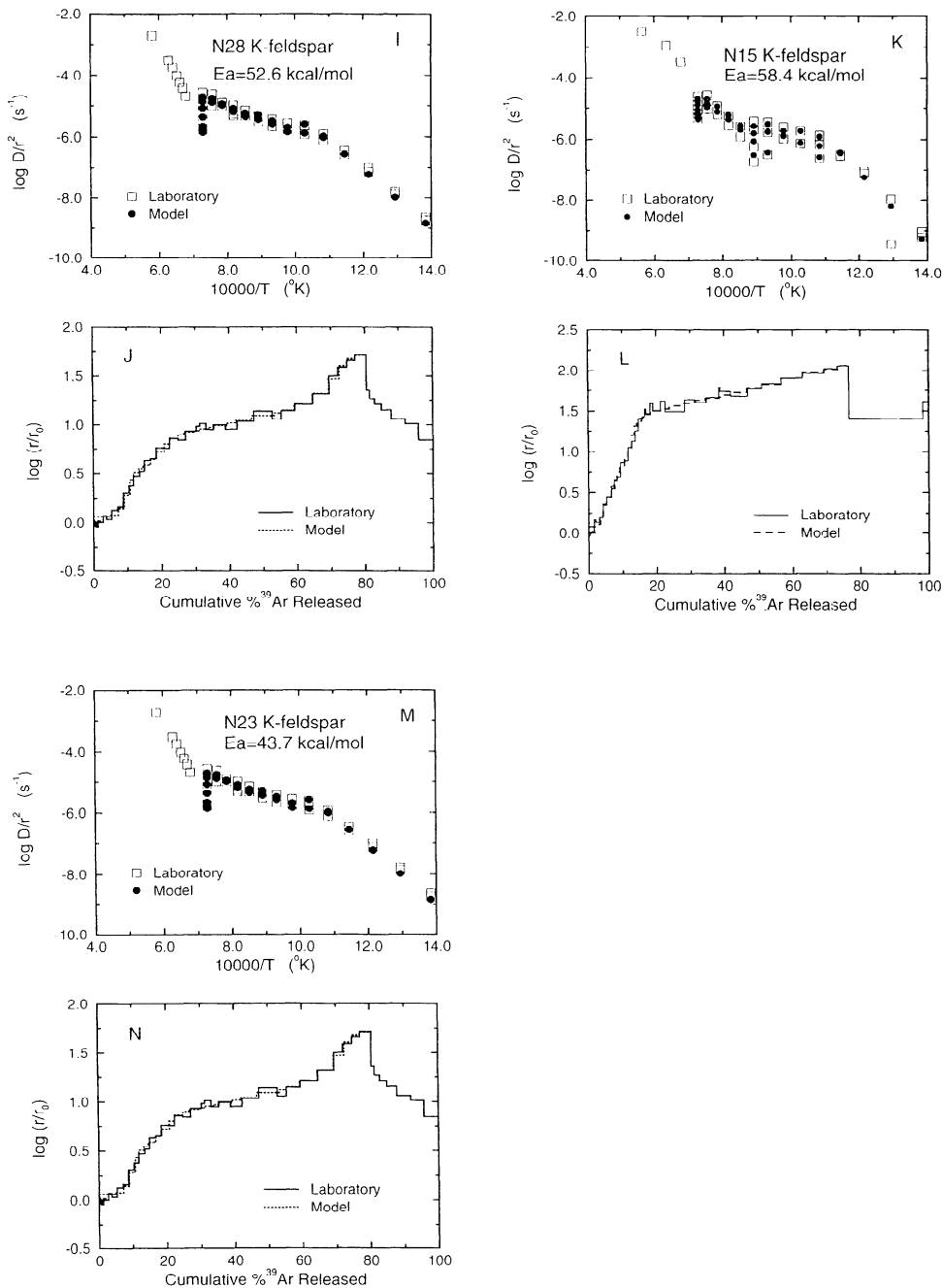


Figure 3. (continued)

450°C to 950°C during the laboratory degassing experiments, and  $\log D/r^2$  generally increased, as might be expected from the dependence of  $D$  upon temperature. The second of each isothermal duplicate run often plots at lower values of  $D/r^2$ . This is consistent with the possibility that effective diffusion length scale was increasing at a given temperature as the experiment progressed. An increase in diffusion length scale with time is consistent with the argon being evolved from a distribution of domains.

During the degassing experiments the smallest domains of the K-feldspars became exhausted of their argon, and the

remaining argon was evolved from progressively larger domains (effective diffusion length scale increased). This increase is best visualized on the " $\log r/r_0$ " plots shown in Figure 3, which are plots of the percent of <sup>39</sup>Ar release (a measure of experiment progress, as in age spectrum diagrams) versus  $\log r/r_0$  (effective diffusion length scale over reference length scale [cf. Lovera *et al.*, 1989]). From zero to >80% of <sup>39</sup>Ar released, the effective diffusion length scales increased by 1.4 to 2.2 orders of magnitude, typical of the length scales resolved by similar experiments [Dunlap *et al.*, 1995]. Note that this range in diffusion length scale is a minimum since the

samples were melted before exhaustion of the largest domains (see also Table 2). Upon melting ( $>1150^{\circ}\text{C}$ ) the apparent diffusion length scale decreased dramatically in every case.

The MDD solutions have either seven or eight domains (Table 2). Although the thermal models below are not sensitive to the number of domains used (the difference between seven and eight is trivial), using fewer domains results in progressively poorer fits, such that using four or fewer domains yields unacceptable fits. The activation energies for the analyses were calculated using the linear, low-temperature portions of the Arrhenius arrays; typically, the first six to eight points are used in least squares regressions. The usual approach is to find the highest activation energy possible [e.g., *Lovera et al.*, 1997], because underestimation of the activation energy results if domains become exhausted within the first few steps of the experiments. Estimated activation energies range from 43.7 to 58.4 kcal/mol (Table 2), with associated errors of less than 2.4 kcal/mol; these values are reasonable for this type of analysis [*Lovera et al.*, 1997].

Some details of the data are worth noting. The unusual dips in the  $\log r/r_0$  plot between 25-80% of gas release for the laboratory results of K-feldspar N31 (Figure 3) indicate a relative decrease in the bulk diffusion length scale. In theory,  $\log r/r_0$  should only increase during the course of the experiments. These decreases, which, in the case of N31 K-feldspar, are associated with age steps that are significantly older than their neighbors, could be caused by melting and/or degassing of populations of inclusions (dips occur at temperatures in excess of  $\sim 900^{\circ}\text{C}$  and when temperature is increased). Similar behavior is exhibited by samples N5 (40-60% of release) and N35 (23-70% of gas release, Figure 3). Another potential cause of the dips in  $\log r/r_0$ , among others, might be degradation of the K-feldspar itself.

## 4.2. Thermal Modeling of K-feldspars

The following discussion of the results of thermal modeling provides a basis for our tectonic interpretations. The main objective of this section is to constrain the times and temperatures at which changes in cooling rate take place.

If the laboratory and model Arrhenius data (see section 4.1) are well matched, then it is possible to model the laboratory age spectrum with two end-member types of thermal histories: (1) continuous cooling and (2) thermal spikes (i.e., one or more thermal pulses). In this exercise we prefer post-Caledonian thermal histories of continuous cooling. The rationale for this is that the southern Norwegian upper crust has not been affected by major orogenic or igneous activity since the Caledonian orogeny, and thus it is unlikely that thermal pulses of significant magnitude have affected the rocks.

At this point it is useful to reiterate that the western part of our traverse was strongly deformed and metamorphosed, mostly in the upper greenschist to amphibolite facies during Caledonian tectonism. All the amphiboles and micas from this region are Caledonian in age, and, since K-feldspars are generally less retentive of their argon, K-feldspars which formed in the Proterozoic should have been completely outgassed of their argon in Caledonian time. This is the case for K-feldspar from the westernmost exposures: samples N1, N35, and N5. However, some K-feldspars from the eastern portion of the traverse preserve pre-Caledonian apparent ages

(N31 and N15), suggesting that the samples were not completely outgassed of argon that accumulated in Proterozoic protoliths. For these samples it might be reasonable to assume that the K-feldspar formed and cooled rapidly at  $\sim 900$  Ma [e.g., *Gorbatschev*, 1985] and then remained below about  $150^{\circ}\text{C}$  until Caledonian reheating. Although this assumption works well for the modeling of N31, it does not for the N15 sample (see section 4.2.6).

**4.2.1. Sample N1.** The young apparent ages and pronounced age gradient exhibited by the age spectrum for N1 K-feldspar (Figure 2a) indicate that final closure of the smallest domains did not occur until  $\sim 270$  Ma. As  $^{40}\text{Ar}/^{39}\text{Ar}$  plateau ages for amphiboles from the Øygarden Complex are as young as 404 Ma, it is odd that the K-feldspar still retains maximum ages of about 430 Ma. The shape of the age spectrum is not suggestive of excess argon, but contamination seems likely in view of the young amphibole results. For the modeling, however, we have assumed that the sample cooled rapidly to below the closure temperatures of the largest domains ( $\sim 350^{\circ}\text{C}$ ) at  $\sim 430$  Ma. Regardless of when cooling to less than  $\sim 350^{\circ}\text{C}$  occurs, little else can be gleaned about the Caledonian thermal history. Model runs with an increased cooling rate, or a thermal spike, at about 400 Ma do not provide better fits than a history of cooling at a constant rate of  $\sim 1^{\circ}\text{C}/\text{Ma}$  over the entire time interval of 430 Ma to 270 Ma (Figure 2b, solid line). Poor fits result from keeping the model isothermal in the 400-300 Ma period, which runs contrary to the results for most of the other samples studied here.

**4.2.2. Sample N35.** The age spectrum for N35 K-feldspar (Figure 2c) indicates that the sample started to accumulate radiogenic argon about 390 Ma after extensional collapse and unroofing of this part of the orogen had already started. Final closure to argon loss did not occur until about 264 Ma.

The Krossnes granite probably cooled rapidly upon emplacement  $\sim 430$  Ma. However, the island arc/ophiolite complex, with which the granite has preserved intrusive contacts, was exposed and covered by a sedimentary sequence [*Thon*, 1985] prior to deformation in the uppermost greenschist to lower amphibolite facies. No other thermochronological constraints are available. Despite this complex history it is clear from the age spectrum that the sample remained hot until  $\sim 390$  Ma. Rapid cooling at  $390 \pm 5$  Ma provides good model fits, which are broadly consistent with the findings of *Fossen and Dunlap* [1998], whereupon cooling to below about  $280^{\circ}\text{C}$  must occur. A final phase of rapid cooling must start at about  $280 \pm 5$  Ma. A temperature drop of about  $80^{\circ}\text{C}$  is required at this time to close the smallest domains to any further argon loss by  $\sim 264$  Ma.

**4.2.3. Sample N5.** The N5 K-feldspar yields apparent ages in the range 275-460 Ma (Figure 2e). Good model fits for N5 K-feldspar require rapid cooling at  $\sim 445$  Ma to fix the age of the largest domain and, after an intervening isothermal period, another cooling event at about 330 Ma (Figure 2f "cold"). This thermal history is at odds with  $^{40}\text{Ar}/^{39}\text{Ar}$  mica ages for the Bergsdalen Nappes that cluster around 400 Ma, indicating cooling to below about  $300^{\circ}\text{C}$ - $350^{\circ}\text{C}$  [*Fossen and Dunlap*, 1998]. The problem is that the calculated closure temperature for the largest (445 Ma) model domain of N5 is only  $\sim 350^{\circ}\text{C}$  (Table 2). However, if excess argon has elevated the apparent age of the largest domains preferentially [*Foster et al.*, 1990], then a hotter thermal history, one more consistent with the

mica data, might be reasonable. If rapid cooling about 400 Ma is imposed, then model fits are poor beyond ~40% of gas release (Figure 2e and 2f "hot"), but at least the model is consistent with available constraints. The post-Caledonian thermal history requires about 70 Ma of extremely slow cooling followed by a relatively rapid cooling event starting about  $330 \pm 10$  Ma, whereupon temperature must drop by at least 50°C. When compared to the results for the other K-feldspars in this study, the 330 Ma model event is the oldest of the group, and the cooling rate is the fastest of the Permian-Carboniferous model rates by about an order of magnitude.

**4.2.4. Sample N31.** K-feldspar N31 yields an age spectrum with maximum ages that are Proterozoic (Figure 2g); thus we assume that a reheating type history is appropriate. There is a family of Caledonian reheating curves that can account for the oldest ages in the N31 spectrum. To be consistent with the available  $^{40}\text{Ar}/^{39}\text{Ar}$  cooling information for micas at ~400 Ma and the indications that thrusting of the Jotun Nappe started at 450 Ma or earlier [Fossen and Dunlap, 1998], two example thermal histories have been calculated where the Jotun Nappe remains hot from ~450 Ma to 390 Ma (Figure 2h). For a broad flat-topped thermal pulse sustained throughout the Caledonian Orogeny (tens of millions of years), maximum temperature is about 320°C (Figure 2h bold line). In consideration of the partially reset amphibole, which suggests temperatures in the lower amphibolite facies, a thermal history with a thermal spike at ~460 Ma (fine line) also yields a good fit when a temperature spike of 390°C is used, but imposing higher temperatures makes it impossible to match age steps older than 450 Ma because the largest domains are outgassed. One possibility is that the largest domains of the K-feldspar are affected by excess argon, and if the >450 Ma ages are discounted, then a more intense thermal spike at ~450 Ma, as suggested by the amphibole, is possible. The thermal history subsequent to about 400 Ma is poorly constrained because of the relatively poor fit between the model and the laboratory results (Figure 3h).

**4.2.5. Sample N28.** The age spectrum for K-feldspar N28 (Figure 2i) suggests that complete outgassing of any potential Proterozoic signature occurred during Caledonian reheating. The ~450 Ma maximum age, however, indicates that the largest domains may be more retentive than the nearby micas, which yield ~400 Ma ages, and that the 550°C maximum suggested by Griffin *et al.* [1985] was reached prior to this time. Consequently, we start the model with zero argon concentration at 460 Ma and cool the sample to below the closure temperature of the largest domain (~350°C) by ~450 Ma and close the intermediate domains by about 400 Ma by cooling through approximately mica closure temperatures. The post-Caledonian thermal history must then remain below this temperature so that the larger domains remain closed.

Correction for chlorine-correlated excess argon was successful. As shown in Figure 4, the applied correction ( $^{40}\text{Ar}_{\text{ex}}/\text{Cl} = 3.0 \times 10^{-6}$ ) completely eliminates the elevated apparent ages in the first 20% of gas release. The smooth rise in apparent ages seen from the second of each isothermal pair of steps is nicely reinforced by the chlorine-corrected ages, such that the slope of the age spectrum from 240 to 300 Ma can be inverted into a cooling rate with confidence.

For a continuous slow cooling model an increase in cooling rate is required at both the onset of Caledonian collapse and,

after an intervening isothermal period, in the Permian. The magnitude of the temperature drop at ~400 Ma must be at least 40°C in order to preserve the ~450 Ma oldest ages in the spectrum. The onset of the next phase of rapid cooling is well constrained at  $280 \pm 10$  Ma. The magnitude of the associated temperature drop is within the range  $75 \pm 25^\circ\text{C}$ . A cooling rate of 3°C/Ma provides the best fit. After about 250 Ma the cooling rate must decrease to match the first 10% of gas release; this result matches nicely with the available fission track data, which indicates that the rocks were hotter than fission track annealing temperatures in apatites at ~160 Ma but were near the surface by about 120 Ma [Rohrman *et al.*, 1995].

**4.2.6. Sample N15.** The age spectrum for K-feldspar N15 exhibits Proterozoic apparent ages (Figure 2k), indicating that the Caledonian temperature peak related to overthrusting (~300°-350°C [cf. Fossen and Dunlap, 1998]) was insufficient to fully outgas the K-feldspar. K-feldspar N17 of Fossen and Dunlap [1998], from the "sparagmites" along the basal portion of the Jotun Nappe Complex to the NE, also exhibits pre-Caledonian ages, which further supports the partial outgassing hypothesis.

As outlined in section 2, we have tried to accommodate the ~900 Ma high-temperature metamorphism, the neo-Proterozoic sedimentation, and the ~415 Ma temperature increase proposed by Fossen and Dunlap [1998]. However, using these constraints, it is not possible for the model age spectrum to closely match the laboratory age spectrum. In the high-temperature portion of the spectrum, from 20-84% of gas release

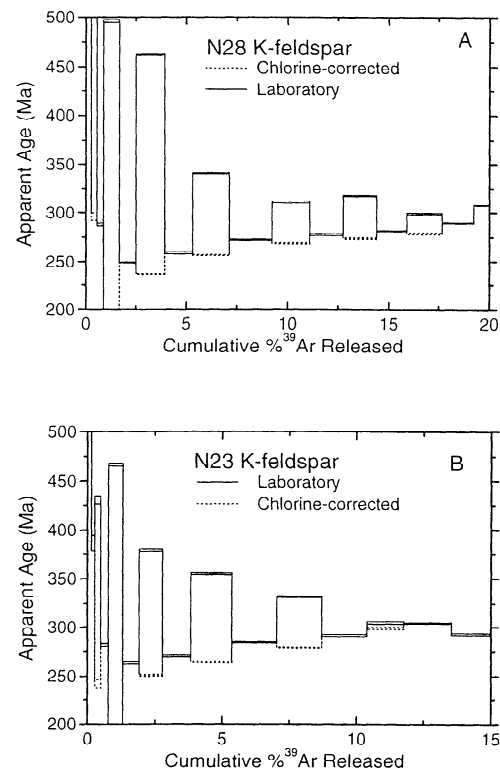


**Figure 4.** Age spectra plot showing difference between uncorrected laboratory ages of first of each isothermal pair of steps for (a) K-feldspar N28 and (b) K-feldspar N23. Ages are corrected for chlorine-correlated excess argon after the method of Harrison *et al.* [1993].

a close fit (not shown) is only possible if the notion of Caledonian reheating is discarded, because the bulk of the ages are Proterozoic. The reason for this may be excess argon contamination of the larger domains, which may be indicated by the pronounced concave-down shape from 20-84% release [Foster *et al.*, 1990].

The Caledonian metamorphism reached lower greenschist facies conditions at this site. If any ~550 Ma apparent ages are to be retained in the model, the maximum temperature attained during a ~415 Ma thermal spike of 5 m.y. duration is about 380°C (Figure 2l). Similarly, the maximum temperature cannot exceed ~400°C for a thermal spike of 1 m.y. in duration. Interestingly, *Nickelsen et al.* [1985] used conodonts from a nearby unit to estimate maximum Caledonian temperatures of 300°-400°C. Although maximum temperature of a thermal spike is reasonably constrained by our analysis, the timing is not. Shifting the thermal spike in time by  $\pm 20$  m.y. still provides fits similar to that in Figure 2k. This indicates little control on the exact timing of the Caledonian thermal spike. After the ~415 Ma thermal spike the sample must be maintained at ~280°C until  $290 \pm 5$  Ma, whereupon the cooling rate must become ~2.4°C/Ma for good model fits.

In summary, an increase in temperature cannot occur in Caledonian time if the laboratory age spectrum is to be matched. In view of the likelihood of the Caledonian temperature increase, however, excess argon must be contaminating the largest domains in the 20-85% portion of gas release.

**4.2.7. Sample N23.** The age spectrum of sample N23 exhibits Paleozoic apparent ages <~400 Ma (Figure 2m), reflecting the higher Caledonian metamorphic grade (middle to upper greenschist facies) along the NW margin of the Jotun Nappe relative to exposures in the SE (N15, lower greenschist facies). Because the arkosic protolith of N23 was deposited in the late Proterozoic, the K-feldspar must have been completely outgassed at ~400 Ma.

*Fossen and Dunlap* [1998] found that white micas from sample N23 gave a discordant  $^{40}\text{Ar}/^{39}\text{Ar}$  age spectrum with apparent ages ranging from 404 to 419 Ma. Thus the middle greenschist facies shearing occurred prior to ~404 Ma. As 395 Ma is the oldest age step evolved from N23 K-feldspar, it would appear that collapse of the Caledonian orogenic wedge resulted in cooling of the N23 site to below the closure temperature of the largest domains in K-feldspar.

The post-Caledonian thermal history of site N23 can be modeled using the laboratory age spectrum corrected for chlorine-correlated excess argon (Figures 2m and 4b). The difference in Cl/K and  $^{40}\text{Ar}/\text{K}$  between isothermal duplicate

steps yields a correlation where  $^{40}\text{Ar}_{\text{ex}}/\text{Cl} = 2.1 \times 10^{-5}$ . This composition has been used to correct the ages of the first step in each isothermal pair, but the ages derived in this way are quite sensitive to the nuclear production ratios ( $^{38}\text{Ar}_{\text{K}}/^{39}\text{Ar}_{\text{K}}$ ) and ( $^{38}\text{Ar}_{\text{Cl}}/^{39}\text{Ar}_{\text{K}}$ ) such that the corrected ages are not known to within about 10%. However, the corrected ages reinforce the age gradient defined by the uncorrected ages alone.

The best fit slow cooling model age spectrum (Figure 2m) shows good agreement with the laboratory age spectrum, except in the interval of 50-70% of gas release where excess argon may be elevating the laboratory age. The timing of changes in cooling rate are well defined (Figure 2n). Sensitivity testing indicates that rapid cooling occurred at both  $400 \pm 5$  Ma and  $300 \pm 5$  Ma. The cooling rate at ~300 Ma must increase from essentially 0° to 4.4 °C/Ma. In addition, the model is quite sensitive to changes in temperature such that changes of only 5°C result in poor fits. According to the model the rocks must remain at about  $140^\circ \pm 5^\circ\text{C}$  until at least 250 Ma for good model fits of the lowest temperature portion of the age spectrum, which is consistent with regional fission track data (discussed in section 5).

## 5. Discussion and Interpretation

The important results of the modeling are compiled in Table 3, which lists the timing of the onset of relatively rapid Devonian cooling, the maximum interim temperatures that can be sustained for continuous slow cooling models, and the minimum temperature drops and best fit cooling rates for the interval 330-250 Ma. The results are displayed graphically in Figure 5, and a tectonic model is presented in cross-sectional form in Figure 6.

Although much more data are needed for firm conclusions, the new analytical data indicate a relatively uniform exhumation history along the 250 km traverse. The K-feldspar thermal models reveal two periods of relatively rapid cooling, one at the end of the Caledonian Orogeny and another in Permo-Carboniferous time (~330-270 Ma). An interim period of thermal stability is also consistent with the data. Six of the seven K-feldspar models yield information about the onset of late Caledonian rapid cooling. Furthermore, the maximum interim temperature and the onset of Permo-Carboniferous rapid cooling are constrained by six models.

### 5.1. Lower Paleozoic Orogeny and Rapid Cooling

The majority of the Caledonian (~450-400 Ma) tectonothermal history is recorded in the age gradients of K-

**Table 3.** Summary of Thermal Modeling Results

Sample	Permo-Carb Temp Drop, °C	Permo-Carb Cool Rate, °C/Ma	Onset of Permo- Carb Rapid Cooling, Ma	Onset of Late- Caledonian Rapid Cooling, Ma	Maximum Sustained Post-Caledonian Temperature, °C
N1	na	na	$270 \pm 30$	$400 \pm 30$	$290 \pm 30$
N5	50	50	$330 \pm 10$	$400 \pm 30$	$300 \pm 30$
N15	90	2.4	$290 \pm 5$	$415 \pm 30^*$	$280 \pm 10$
N23	100	4.4	$300 \pm 5$	$400 \pm 5$	$250 \pm 10$
N28	75	3.0	$280 \pm 10$	$400 \pm 20$	$270 \pm 10$
N31	na	na	na	$380 \pm 20$	na
N35	80	4.0	$280 \pm 5$	$390 \pm 5$	$280 \pm 10$

Permo-Carb, Permo-Carboniferous; na, not available, \* Value from N17 K-feldspar of Fossen and Dunlap [1998].

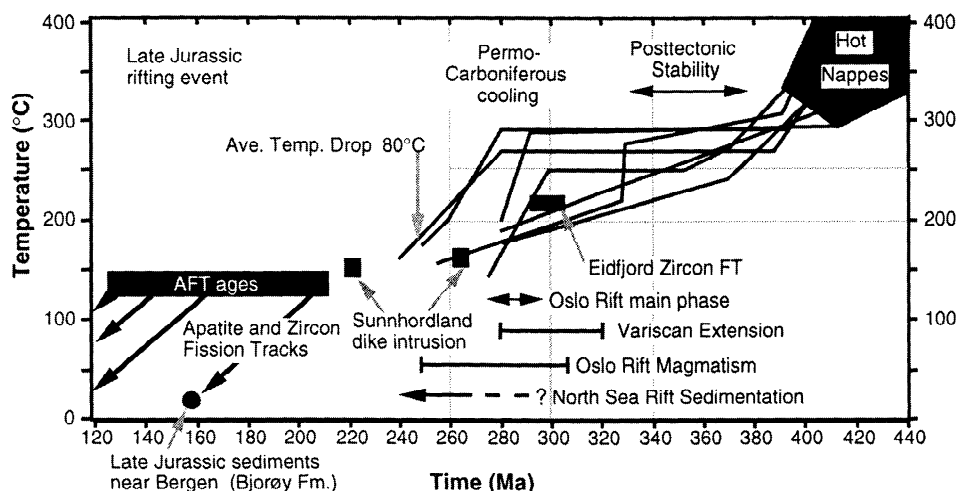


**Figure 5.** Post-Caledonian thermal history; plot of temperature versus time summarizing the results of multiple diffusion domain thermal modeling of K-feldspar  $^{40}\text{Ar}/^{39}\text{Ar}$  data. "Ave Temp Drop 80°C" is the amount by which temperature must decline during the Permo-Carboniferous rapid cooling ( $\sim 80^\circ\text{C}$ ) to obtain good model fits. Eidfjord data arc from *Andriessen and Bos* [1986]. Time spans of significant tectonic events are as follows: Sunnhordland dyke date is from *Lovelie and Mitchell* [1982]. Oslo rift main phase is from *Neumann et al.* [1992]. Time span for Oslo rift magmatism from *Sundvoll et al.* [1990]. Time span for Variscan extensional phase is from *Costa and Rey* [1995]. Onset of North Sea sedimentation is estimated [e.g., *Rohrman*, 1996].

feldspars N15, N28, and N31 (Figures 6a, 6b, and 6c). Although K-feldspar N5 also exhibits Caledonian ages, we suspect that this is due to excess argon contamination (micas and amphiboles are younger, in general), so we prefer the "hot" thermal history for N5 (Figure 2f). Whereas the eastern portion of the traverse (N15) remained relatively cool ( $< 350^\circ\text{C}$ ) during Caledonian thrusting (Figure 6a), K-feldspar N23, which yielded maximum ages of  $\sim 395$  Ma, indicates Caledonian temperatures high enough to completely outgas Proterozoic crystals. These results along with that for N28 support the interpretation of a Caledonian thermal gradient which increased toward the NW across the Jotun Nappe. All of the above findings are consistent with the previous  $^{40}\text{Ar}/^{39}\text{Ar}$  study of *Fossen and Dunlap* [1998], who found that the latest phase of Caledonian rapid cooling occurred during extensional collapse of the orogen which culminated subsequent to 400 Ma (Figure 6c).

## 5.2. Middle Paleozoic Stability

The time interval of  $\sim 380$ -330 Ma appears to be one of tectonic and thermal stability in the interior of southern Norway. If the result for N5 is significantly affected by excess argon, then stability may have lasted until  $\sim 300$  Ma (note also the unusually high cooling rate of  $\sim 53^\circ\text{C}/\text{Ma}$  at 330 Ma). The maximum possible sustained temperatures of  $250^\circ$ - $300^\circ\text{C}$  for the K-feldspars in the 380-300 Ma time interval (Figure 5 and Table 3) indicate that the presently exposed crust resided at similar depths (assuming a uniform geothermal gradient). It follows that exhumation since that time has been, according to our level of resolution, essentially uniform across the traverse. Further support comes from the  $\sim 300$  Ma zircon fission track ages from the Eidfjord region (closure at  $220^\circ\text{C}$ ? [*Andriessen and Bos*, 1986]).

Tectonic stability in this interval is also supported by the lack of evidence for metamorphism or significant deformation or sedimentation involving the southern Norwegian crust. Field observations [*Fossen*, 1998] and dating of fault rocks (R.B. Pedersen, unpublished data, 1997) in the study area indicate that much of the faulting activity is of (Lower) Devonian age, formed during the last part of the postcontractual cooling (collapse) event when temperatures crossed the brittle-ductile transition ( $\sim 300^\circ$ - $350^\circ\text{C}$  for granitic rock [e.g., *Davis and Reynolds*, 1996]). Later local reactivation of faults demonstrably occurred in the Permian and late- or post-Jurassic [*Fossen et al.*, 1997], in particular along the Nordfjord-Sogn detachment [*Eide et al.*, 1997] and the offshore Øygarden Fault Complex (Figure 1) [*Fossen* 1998]. In contrast, continuous cores collected during an ongoing subsea tunnel project through the HSZ reveal surprisingly little reactivation of the original, ductile structure. Similarly, the décollement zone between the Caledonian orogenic wedge and the basement was inactive during the Lower Devonian ductile extensional deformation (Figure 6c) and bears no sign of later reactivation. It therefore seems likely that any perturbation of the K-Ar system by faulting or fault reactivation and associated heat sources is of local importance only. All samples collected for this study were collected away from fault structures so that local effects of faulting or fault reactivation were avoided.

If the whole of southern Norway was, indeed, tectonically stable during the time interval 380-330 Ma or possibly 380-300 Ma, then it must have stabilized between two topographic extremes: (1) a stable, remnant, possibly mature landscape standing topographically high (1.5 km on average?) as a result of a persistent overthickness of crust relative to the mantle lithosphere or (2) a deeply eroded and highly extended Caledonian orogen lying close to sea level because of an

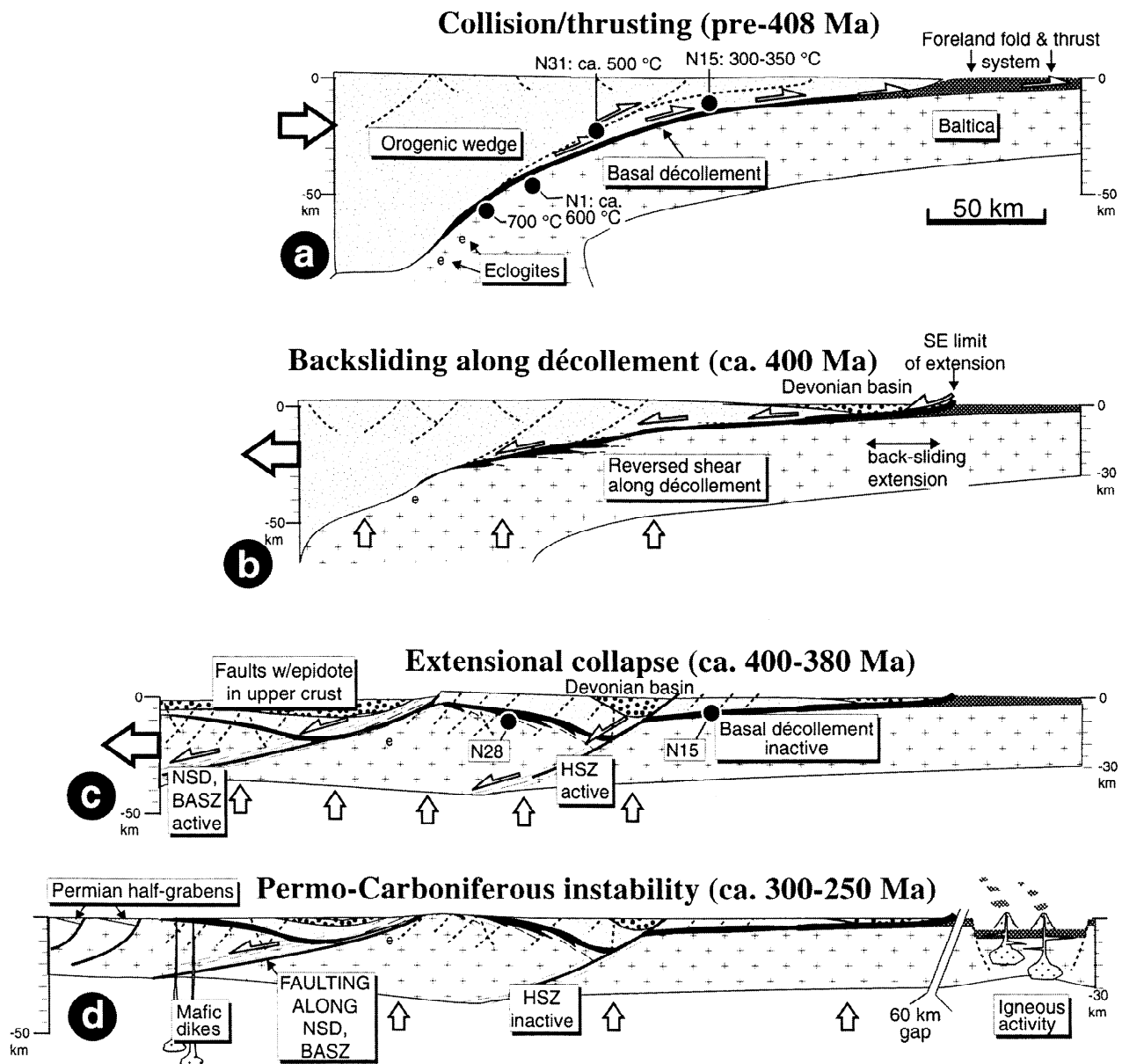


**Figure 6.** Highlights of the Paleozoic development of the southern Norwegian crust (schematic profile based on profiles shown in Figure 1): (a) Caledonian collisional stage, (b) Early Devonian NW directed transport of orogenic wedge, (c) extension by northwest dipping shear zones followed by faulting as the crust is cooled, and (d) Permian rifting and magmatism in the Oslo rift and dike intrusion near the western coast. Note exhumation of crust in continental interior. The profile in Figure 6d has been extended slightly to the west to show the development of Permian half grabens [e.g., *Rohrman et al.*, 1996, and references therein] and to the east to show the Oslo Graben.

underthickness of crust relative to mantle lithosphere. The present-day crustal thickness of about 30-40 km [Kinck *et al.*, 1993] is "normal," indicating that the crust was thicker in the 380-330 Ma interval and has thinned mainly by erosion since that time (~9 km for a geothermal gradient of 30°C/km). Another observation supporting scenario 1 is that the crust along our traverse was extended during late orogenic collapse, but it was not highly extended [Fossen, 1992]. If an overthickness of crust was, in fact, sustained, then southern

Norway would have remained topographically high. Moreover, orogenic belts with thick crust may sustain a significant topographic expression for many tens of millions of years if late orogenic extension is not extreme and erosional denudation is extremely slow. Examples of thick crust and associated topography sustained for 50-100 m.y. or more after the cessation of tectonism include the Rockies [Burchfiel *et al.*, 1992; Sheehan *et al.*, 1995], the Appalachians [Long and Liow, 1986; Hatcher, 1992], and the Urals [Echtler *et al.*,

1996]. The preferred scenario for southern Norway is that the crust maintained a significant post-Caledonian topography of ~1.5 km until about 300 Ma.

### 5.3. Late Paleozoic Cooling

In the interval of ~380-250 Ma, differential exhumation between sample sites does not appear to have exceeded 2 km; otherwise, this would be reflected in the K-feldspar data. Despite this apparent thermal uniformity there is some 60 m.y. of diachroneity in the onset of the more rapid Permo-Carboniferous cooling. Although we would prefer to have more than one analysis at each site, let us consider the possibility that this variation is real. The onset of Permo-Carboniferous rapid cooling is earliest at site N5 (Figure 1), and the model cooling rate is the highest of the group by far (50°C/Ma). This cooling may be related to minor reactivation of the BASZ (Fensfjord Fault [Wennberg and Milnes, 1994]), but more data are needed to test this hypothesis. Starting about 300 Ma, increases in model cooling rates are interpreted to occur first in the east at sites N23 and N15, followed closely by cooling at sites N28 and N35 and finally by cooling at site N1 along the western coast. The interpreted cooling rates are in the range of 2°-5°C/Ma, which is exceedingly slow, but is consistent with 1 km of erosion every 6-15 m.y., assuming a uniform unperturbed geothermal gradient of 30°C/km. The mean magnitude of the Permo-Carboniferous temperature drop is  $79^\circ \pm 22^\circ\text{C}$  ( $2\sigma$ ), as tested through five of the seven models.

The onset of Permo-Carboniferous relatively rapid cooling as recorded by the K-feldspars may be related to the onset of rifting in the Oslo Graben and North Sea region (Figures 5 and 6d). Magmatism in the Oslo Graben extends from about 300 Ma to about 240 Ma [Sundvoll *et al.*, 1990]. According to Neumann *et al.* [1992] the Oslo Graben experienced widespread basaltic volcanism from 300 to 295 Ma, followed by the main rifting from 295 to 275 Ma. These time periods correlate with the onset of Permo-Carboniferous rapid cooling in K-feldspar models N1, N15, N23, N28, and N35. Along the west coast of Norway (Figure 6d) a phase of basaltic dike intrusion and, locally, faulting occurred by 260 Ma [Færseth *et al.*, 1976; Løvlie and Mitchell, 1982; Torsvik *et al.*, 1997]. In the North Sea, thick Permo-Triassic clastic sequences were deposited in the half grabens that underlie the Viking Graben and Horda platform [Gabrielsen *et al.*, 1990]. Although the onset of the Permian sedimentation in the North Sea is not precisely known, partially because of a lack of well data, the Permo-Triassic sequences would appear to be up to several kilometers thick [Steel and Ryseth, 1990; Roberts *et al.*, 1995; Færseth *et al.*, 1995]. The source of these sediments is considered to be the Norwegian mainland [e.g., Ziegler, 1990]. The 260-270 Ma zircon fission track ages for grains recovered from wells into Triassic and Jurassic North Sea sediments [Rohrman *et al.*, 1996] are consistent with the detritus being derived from Norwegian mainland basement that cooled through ~220°C in the Permian and was exposed at the surface in Triassic and Jurassic times.

The Permo-Carboniferous exhumation recorded in the K-feldspars is clearly contemporaneous with early-stage rifting in the Oslo Graben. In the absence of tectonic exhumation the data indicate erosional denudation of about  $3 \pm 1$  km of the

southern Norwegian crust (assuming a geothermal gradient of 20°-40°C/km and 80°C of cooling). The large volumes of erosional products must have been deposited in the North Sea, because only very restricted volumes accumulated in the Oslo rift system. Is it possible that the North Sea rift had already started to form by about 300 Ma and was able to accommodate the large clastic flux from the mainland? The onset of extension in the North Sea is very poorly constrained from offshore data but has been considered to be Permo-Triassic [Gabrielsen *et al.*, 1990] or Triassic [Roberts *et al.*, 1995]. However, the results presented here suggest that the rifting history in the North Sea may date back to at least 300 Ma (latest Carboniferous or earliest Permian). This interpretation is in full agreement with results of a regional study of seismic, magnetic, and gravimetric data from the southern North Sea basin [Faleide *et al.*, 1997] and may call for a revision of numerical basin models presented for the North Sea basin [e.g., Roberts *et al.*, 1995].

Erosion of  $3 \pm 1$  km of crust from a topography averaging 1.5 km above sea level could easily be accommodated by isostatic rebound maintaining the eroding crust above sea level [e.g., Stephenson and Lambeck, 1985]. Uplift mechanisms such as delamination of the lower lithosphere (associated with Variscan collision?) or changes in the thermal and/or density structure of the lithosphere could have produced the required topography, but these explanations are perhaps too ad hoc, and there is no supporting evidence. It must be concluded then that the southern Norwegian crust was topographically high at ~300 Ma and that the underlying rocks were exhumed as a result of rifting at the continental margin (Figure 6d), lowering of the base level, and relatively rapid erosional downcutting (~0.15 mm/yr on average).

## 6. Conclusions

The following main conclusions can be drawn from the K-feldspar thermochronological study of southern Norway: (1) Relatively rapid cooling was associated with extensional collapse of the Caledonian mountain chain starting about 400 Ma (Lower Devonian). (2) The time interval of ~380-330 Ma appears to be one of relative tectonic and thermal stability; this stability may even have extended to ~300 Ma. We suggest that the southern Norwegian crust maintained a significant post-Caledonian topography of ~1.5 km on average during this period, similar to the sustained topography of the present-day Appalachians. (3) Most of the K-feldspars sampled along a 250 km E-W traverse of southern Norway experienced renewed cooling at a few °C/Ma in the time interval 300-250 Ma. (4) Cooling of the southern Norwegian crust in the late Paleozoic (~300-250 Ma) is interpreted to be the result of fairly uniform exhumation across the traverse. The exhumation is interpreted to be the result of rifting in the Oslo Graben and North Sea basin, lowering of the base level, and an increase in the rate of erosional downcutting. (5) The K-feldspar thermal models indicate that, in the presently exposed crust, temperatures dropped to those of apatite fission track retention after 250 Ma, which is in accord with published apatite fission track data from the region [Rohrman *et al.*, 1996]. (6) The K-feldspar thermochronology of southern Norway provides a continuous time-temperature history from Late Caledonian

orogenic collapse, through a likely period of tectonic and thermal stability, with final closure to diffusive loss of argon occurring mainly after the commencement of rifting at ~300 Ma.

## Appendix: Analytical Procedure

Mineral separation was by routine heavy liquid, flotation, and magnetic methods, and a final purity of better than 99% was achieved in most cases. The main impurities are populations of mineral and fluid inclusions. K-feldspars fragments were sized (150-420  $\mu\text{m}$  range) after crushing using mesh sieves. See supplementary data tables for details.

Analytical procedure for  $^{40}\text{Ar}/^{39}\text{Ar}$  analysis of samples measured at The Australian National University is covered by Dunlap *et al.* [1995]. The remaining samples were analyzed at the University of California, Los Angeles; the analytical procedures outlined below were used.

The samples were irradiated for 80 hours (without cadmium shielding) in the Ford Reactor, University of Michigan, to attain a neutron fluence similar to previously run samples. Aside from different time-temperature schedules for step heating, treatment of the data was essentially identical to that done at The Australian National University.

Temperature was monitored by a thermocouple at the base of a tantalum crucible within a double-vacuum resistance furnace. Experiments were started at 450°C and concluded at 1500°C. Step heating schedules are listed in the supplementary data

tables. At each extraction temperature the gas released was exposed to Zr-Al getter pumps to remove active gases, and the argon was subsequently isotopically analyzed using a VG1200 gas source mass spectrometer operated in the static mode. Measurements were made with an electron multiplier (Ar sensitivity of about 5E-17 mol/mV). Getter section blanks were normally below 5E-16 mol on mass 40 for static collection over 10 min. Blanks were atmospheric, as well as could be determined, and the mass 39 blank (10 min) was normally below 2E-18 mol. Furnace blanks below 1000°C were generally well below 5E-15 mol of  $^{40}\text{Ar}$ . The  $^{40}\text{K}$  abundance and decay constants recommended by the International Union of Geological Sciences Subcommittee on Geochronology were used [Steiger and Jager, 1977]. See supplementary data tables for correction factors and flux monitor information.

**Acknowledgments.** We thank the Australian Nuclear Science and Technology Organization and the Australian Institute of Nuclear Science and Engineering for irradiations. We have had significant discussions relating to this work with Ian McDougall and Peter van der Beek of The Australian National University, Research School of Earth Sciences. This project could not have been concluded without both the support of a U.S. National Science Foundation Postdoctoral Fellowship and the favorable environment provided by Mark Harrison and his argon mercenaries at UCLA. We are grateful for reviews by T. Boundy and in particular by E. Eide.

## References

- Andersen, T.B., B. Jamtveit, J.F. Dewey, and E. Swenson, Subduction and exhumation of continental crust: Major mechanisms during continent-continent collision and orogenic extensional collapse, a model based on the Norwegian Caledonides, *Terra Nova*, 3, 303-310, 1991.
- Andriessen, P.A.M., and A.B. Bos, Post-Caledonian thermal evolution and crustal uplift in the Eidfjord area, western Norway, *Nor. Geol. Tidsskr.*, 66, 243-250, 1986.
- Baldwin, S.L., M.T. Harrison, and J.D. Fitz Gerald, Diffusion of  $^{40}\text{Ar}$  in metamorphic hornblende, *Contrib. Mineral. Petrol.*, 105, 691-703, 1990.
- Berry, H.N., D.R. Lux, A. Andresen, and T.B. Andersen, Progressive exhumation during orogenic collapse as indicated by  $^{40}\text{Ar}/^{39}\text{Ar}$  cooling ages from different structural levels, southwest Norway, *Geonytt*, 22, 20-21, 1995.
- Boundy, T.M., E.J. Essene, C.M. Hall, H. Austrheim, and A.N. Halliday, Rapid exhumation of lower crust during continent-continent collision and late extension: Evidence from  $^{40}\text{Ar}/^{39}\text{Ar}$  incremental heating of hornblendes and muscovites, Caledonian Orogen, western Norway, *Geol. Soc. Am. Bull.*, 108, 1425-1437, 1996.
- Bryhni, I., K. Brastad, and V. Jacobsen, Subdivision of the Jotun Nappe Complex between Aurlandsfjorden and Nørøyfjorden, south Norway, *Bull. Nor. Geol. Unders.*, 380, 23-33, 1983.
- Burchfiel, B.C., D.S. Cowan, and G.A. Davis, Tectonic overview of the Cordillera orogen in the western United States, in *The Geology of North America*, vol. G-3, *The Cordillera Orogen, Conterminous United States*, edited by B. C. Burchfiel, P. W. Lipman, and M. L. Zoback, pp. 407-479, Geol. Soc. Am., Boulder, Colo., 1992.
- Chauvet, A., and R.D. Dallmeyer,  $^{40}\text{Ar}/^{39}\text{Ar}$  mineral dates related to Devonian extension in the southwestern Scandinavian Caledonides, *Tectonophysics*, 210, 155-177, 1992.
- Corfu, F., U-Pb and Rb-Sr systematics in a polyorogenic segment of the Precambrian shield, central southern Norway, *Lithos*, 13, 305-323, 1980.
- Costa, S., and P. Rey, Lower crustal rejuvenation and growth during post-thickening collapse: Insights from a crustal cross section through a Variscan metamorphic core complex, *Geology*, 23, 905-908, 1995.
- Dallmeyer, R.D., L. Johansson, and C. Möller, Chronology of Caledonian high-pressure granulite-facies metamorphism, uplift, and deformation within northern parts of the Western Gneiss Region, Norway, *Geol. Soc. Am. Bull.*, 104, 444-455, 1992.
- Davis, G.H., and S.J. Reynolds, *Structural Geology of Rocks and Regions*, 776 pp., John Wiley, New York, 1996.
- Dunlap, W. J., Neocrystallization or cooling?:  $^{40}\text{Ar}/^{39}\text{Ar}$  ages of white micas from low grade mylonites, *Chem. Geol.*, 143, 181-203, 1997.
- Dunlap, W.J., C. Teyssier, I. McDougall, and S. Baldwin, Thermal and structural evolution of the intracratonic Arltunga Nappe Complex, central Australia, *Tectonics*, 14, 1182-1204, 1995.
- Echtler, H.P., M. Stiller, F. Steinhoff, C. Krawczyk, A. Suleimanov, V. Spiridonov, J. H. Knapp, Y. Menshikov, J. Alvarez-Marron, N. Yunusov, Preserved collisional crustal structure of the southern Urals revealed by vibroseis profiling, *Science*, 274, 224-226, 1996.
- Eide, E., T.H. Torsvik, and T.B. Andersen, Absolute dating of brittle fault movements: Late Permian and late Jurassic extensional fault breccias in western Norway, *Terra Nova*, 9, 135-139, 1997.
- Færseth, R.B., R.M. Macintyre, and J. Naterstad, Mesozoic alkaline dykes in the Sunnhordland region, western Norway: Ages, geochemistry and regional significance, *Lithos*, 9, 331-345, 1976.
- Færseth, R.B., R.H. Gabrielsen, and C.A. Hurich, Influence of basement in structuring of the North Sea basin, offshore southwest Norway, *Nor. Geol. Tidsskr.*, 75, 105-119, 1995.
- Faleide, J.I., R. Myklebut, L. Stuevold, G. Mathisen, and E. Ditcha, Sein-Paleozoisk rifting og magmatisme i Skagerrak, Kattegat og Nordsjøen, *Geonytt*, 24, 34-35, 1997.
- Fossen, H., The Ulriken Gneiss Complex and the Rundemanen Formation: A basement-cover relationship in the Bergen Arcs, West Norway, *Bull. Nor. Geol. Unders.*, 412, 67-86, 1988.
- Fossen, H., The role of extensional tectonics in the Caledonides of South Norway, *J. Struct. Geol.*, 14, 1033-1046, 1992.
- Fossen, H., Structural evolution of the Bergsdalen Nappes, southwest Norway, *Bull. Nor. Geol. Unders.*, 424, 23-30, 1993.
- Fossen, H., Advances in understanding the post-Caledonian structural evolution of the Bergen area, west Norway, *Nor. Geol. Tidsskr.*, 78, 33-36, 1998.
- Fossen, H., and H. Austrheim, Age of the Krossnes Granite, west Norway, *Bull. Nor. Geol. Unders.*, 413, 61-65, 1988.
- Fossen, H., and W.J. Dunlap, Timing and kinematics of Caledonian thrusting and extensional collapse, southern Norway: Evidence from  $^{40}\text{Ar}/^{39}\text{Ar}$  thermochronology, *J. Struct. Geol.*, 20, 765-781, 1998.
- Fossen, H., and E. Rykkelid, Shear zone structures in the Øygarden Complex, western Norway, *Tectonophysics*, 174, 385-397, 1990.
- Fossen, H., and E. Rykkelid, Post-collisional extension of the Caledonide orogen in



- Scandinavia: Structural expressions and tectonic significance, *Geology*, 20, 737-740, 1992.
- Fossen, H., G. Mangerud, J. Hesthammer, T. Bugge, and R. Gabrielsen, The Bjorøy Formation: A newly discovered occurrence of Jurassic sediments in the Bergen Arc System, *Nor. Geol. Tidsskr.*, 77, 269-287, 1997.
- Foster, D.A., T.M. Harrison, P. Copeland, and M.T. Heizler, Effects of excess argon within large diffusion domains on K-feldspar age spectra, *Geochim. Cosmochim. Acta*, 54, 1699-1708, 1990.
- Gabrielsen, R.H., R.B. Færseth, L.N. Jensen, J.E. Kalheim, and F. Riis, Structural elements of the Norwegian continental shelf, I: The Barents Sea region, *Norwegian Petroleum Directorate Bull.*, 6, 33 pp., Stavanger, Norway, 1990.
- Gebauer, D., M.A. Lappin, M. Grunefelder, and A. Wyttenbach, The age and origin of some Norwegian eclogites, *Chem. Geol.*, 52, 227-247, 1985.
- Gorbatschev, R., Precambrian basement of the Scandinavian Caledonides, in *The Caledonide Orogen - Scandinavia and Related Areas*, vol. 1, edited by D. G. Gee and B. A. Sturt, pp. 197-212, John Wiley, New York, 1985.
- Gradstein, F.M., and J. Ogg, A Phanerozoic time scale, *Episodes*, 19, 3-5, 1996.
- Griffin, W.L., H. Austrheim, K. Brastad, I. Bryhni, A.G. Krill, E.J. Krogh, M.B.E. Mørk, H. Quale, and B. Tørudbakken, High-pressure metamorphism in the Scandinavian Caledonides, in *The Caledonide Orogen - Scandinavia and Related Areas*, edited by D.G. Gee and B.A. Sturt, vol. 1, pp. 783-801, John Wiley, New York, 1985.
- Harrison, T. M., M.T. Heizler, and O.M. Lovera, In vacuo crushing experiments and K-feldspar thermochronology, *Earth Planet. Sci. Lett.*, 117, 169-180, 1993.
- Hatcher, R.D., Jr., Tectonic synthesis of the U.S. Appalachians, in *The Geology of North America*, vol. F-2, *The Appalachian-Ouachita Orogen in the United States*, edited by R.D. Hatcher Jr., W.A. Thomas, and G.W. Viele, pp. 511-535, Geol. Soc. Am., Boulder, Colo., 1992.
- Hossack, J.R., and M.A. Cooper, Collision tectonics in the Scandinavian Caledonides, in *Collision Tectonics*, edited by M.P. Coward and A.C. Ries, *Geol. Soc. Spec. Publ.*, 19, 287-304, 1986.
- Kinck, J.J., E.S. Husebye, and F.R. Larsson, The Moho depth distribution in Fennoscandia and the regional tectonic evolution from Archean to Permian times, *Precambrian Res.*, 64, 23-51, 1993.
- Kumpulainen, R., and J.P. Nystuen, Late Proterozoic basin evolution and sedimentation in the westernmost part of Baltoscandia, in *The Caledonide Orogen - Scandinavia and Related Areas*, vol. 1, edited by D.G. Gee and B.A. Sturt, pp. 213-245, John Wiley, New York, 1985.
- Long, L.T., and J.-S. Liow, Crustal thickness, velocity structure, and the isostatic response function in the southern Appalachians, in *Reflection Seismology: The Continental Crust, Geodynamic series*, vol. 14, edited by M. Barazangi and L. Brown, p. 215-222, AGU, Washington, D. C., 1986.
- Lovera, O.M., F.M. Richter, and T.M. Harrison, domain sizes, *J. Geophys. Res.*, 94, 17,917-17,936, 1989.
- Lovera, O.M.R., F.M. Richter, and T.M. Harrison, Diffusion domains determined by  $^{39}\text{Ar}$  released during step heating, *J. Geophys. Res.*, 96, 2057-2069, 1991.
- Lovera, O.M., M. Grove, T.M. Harrison, and K.I. Mahon, Systematic analysis of K-feldspar  $^{40}\text{Ar}/^{39}\text{Ar}$  step heating results. I, Significance of activation energy determinations, *Geochim. Cosmochim. Acta*, 61, 3171-3192, 1997.
- Løvlie, R., and J.G. Mitchell, Complete remagnetization of some Permian dykes from western Norway induced during burial/uplift, *Phys. Earth Planet. Inter.*, 30, 415-421, 1982.
- McDougall, I., and T.M. Harrison, *Geochronology and Thermochronology by the  $^{40}\text{Ar}/^{39}\text{Ar}$  Method*, 212 pp., Oxford Univ. Press, New York, 1988.
- Milnes, A.G., and A.G. Koestler, Geological structure of Jotunheimen, southern Norway (Sognefjell-Valdres cross-section), in *The Caledonide Orogen - Scandinavia and Related Areas*, vol. 1, edited by D.G. Gee and B.A. Sturt, pp. 457-474, John Wiley, New York, 1985.
- Neumann, E.R., K.H. Olsen, W.S. Baldrige, and B. Sundvoll, The Oslo Rift: A review, *Tectonophysics*, 208, 1-18, 1992.
- Nickelsen, R.P., J.R. Hossack, M.R. Garton, and J. Repetsky, Late Precambrian to Ordovician stratigraphy and correlation in the Valdres and Synnfjell thrust sheets of the Valdres area, southern Norwegian Caledonides, with some comments on sedimentation, in *The Caledonide Orogen - Scandinavia and Related Areas*, vol. 1, edited by D.G. Gee and B.A. Sturt, pp. 369-378, John Wiley, New York, 1985.
- Norton, M., Late Caledonian extension in western Norway: A response to extreme crustal thickening, *Tectonics*, 5, 192-204, 1986.
- Olaussen, F., B.T. Larsen, and R. Steel, The upper Carboniferous-Permian Oslo rift: Basin fill in relation to tectonic development, in *Pangea: Global Environments and Resources*, Mem. Can. Soc. Pet. Geol., 17, 175-197, 1994.
- Osmundsen, P.T., and T.B. Andersen, Caledonian compression and late-orogenic extensional deformation in the Staveneset area, Sunnfjord, western Norway, *J. Struct. Geol.*, 16, 1385-1401, 1994.
- Pringle, I.R., A. Kvale, and L.B. Anonsen, The age of the Hernes granite, Lower Bergsdalen Nappe, western Norway, *Nor. Geol. Tidsskr.*, 55, 191-195, 1975.
- Richter, F.M., O.M. Lovera, T.M. Harrison, and P. Copeland, Tibetan tectonics from  $^{40}\text{Ar}/^{39}\text{Ar}$  analysis of a single K-feldspar sample, *Earth Planet. Sci. Lett.*, 105, 266-278, 1991.
- Riis, F., Quantification of Cenozoic vertical movements of Scandinavia by correlation of morphological surfaces with offshore data, *Global Change*, 12, 331-357, 1996.
- Roberts, A.M., G. Yielding, N.J. Kusznir, I.M. Walker, and D. Dorn-Lopez, Quantitative analysis of Triassic extension in the northern Viking Graben, *Geol. Soc. Spec. Publ.*, 152, 15-26, 1995.
- Rohrman, M., P. van der Beek, P. Andriessen, and S. Cloetingh, Meso-Cenozoic morphotectonic evolution of southern Norway: Neogene domal uplift inferred from apatite fission track thermochronology, *Tectonics*, 14, 704-718, 1995.
- Rohrman, M., P.A.M. Andriessen, and P.A. van der Beek, The relationship between basin and margin thermal evolution assessed by fission track thermochronology: An application to offshore southern Norway, *Basin Res.*, 8, 45-63, 1996.
- Schärer, U., U-Pb and Rb-Sr dating of a polymetamorphic nappe terrain: The Caledonian Jotun Nappe, southern Norway, *Earth Planet. Sci. Lett.*, 49, 205-218, 1980.
- Sheehan, A.F., G.A. Abers, C.H. Jones, and A.L. Lerner-Lam, Crustal thickness variations across the Colorado Rocky Mountains from teleseismic receiver functions, *J. Geophys. Res.*, 100, 20,391-20,404, 1995.
- Steel, R., and A. Ryseth, The Triassic - Early Jurassic succession in the northern North Sea: Megasequence stratigraphy and intra-Triassic tectonics, in *Tectonic Events Responsible for Britain's Oil and Gas Reserves*, edited by R.F.P. Hardman and J. Brooks, *Geol. Soc. Spec. Publ.*, 55, 139-168, 1990.
- Steiger, R., and E. Jaeger, Subcommission on geochronology: Convention on the use of decay constants in geo- and cosmochronology, *Earth Planet. Sci. Lett.*, 36, 359-362, 1977.
- Stephenson, R., and K. Lambeck, Erosion-isostatic rebound models for uplift: An application to south-eastern Australia, *Geophys. J. R. Astron. Soc.*, 82, 31-55, 1985.
- Sundvoll, B., E.R. Neumann, B.T. Larsen, and E. Tuen, Age relations among the Oslo Rift magmatic rocks: Implications for tectonic and magmatic modelling, *Tectonophysics*, 178, 67-87, 1990.
- Thon, A., Late Ordovician and Early Silurian cover sequences to the west Norwegian ophiolite fragments: Stratigraphy and structural evolution, in *The Caledonide Orogen - Scandinavia and Related Areas*, vol. 1, edited by D.G. Gee and B.A. Sturt, pp. 407-415, John Wiley, New York, 1985.
- Torsvik, T.H., T.B. Andersen, E.A. Eide, and H.J. Walderhaug, The age and tectonic significance of dolerite dykes in Western Norway, *J. Geol. Soc. Lond.*, 154, 961-973, 1997.
- Wennber, O.P., and A.G. Milnes, Interpretation of kinematic indicators along the northeastern margin of the Bergen Arc System: a preliminary field study, *Nor. Geol. Tidsskr.*, 74, 166-173, 1994.
- Ziegler, P.A., Tectonic and palaeogeographic development of the North Sea rift system, in *Tectonic Evolution of the North Sea Rifts*, edited by D.J. Blundell and A.D. Gibbs, pp. 1-36, Clarendon, Oxford, England, 1990.

W.J. Dunlap, Research School of Earth Sciences, The Australian National University, Canberra ACT 0200, Australia. (email: Jim.Dunlap@anu.edu.au)

H. Fossen, Department of Geology, University of Bergen, Allegt. 41, N-5007 Bergen, Norway. (email: haakon.fossen@geol.uib.no)

(Received October 24, 1997;  
revised April 23, 1998;  
accepted May 12, 1998)